

# Oxidation of ferrocenyl ketones using selenium(IV) oxide: Crystal and molecular structures of racemic 2,3-diferrocenyl-1,4-diphenylbutane-1,4-dione, racemic and meso 2,3-diferrocenyl-1,4-bis(4-biphenyl) butane-1,4-dione, and ferrocenylmethyl(4-biphenyl) ketone

S. Zaka Ahmed, Christopher Glidewell<sup>\*</sup>, Philip Lightfoot

*School of Chemistry, University of St Andrews, St Andrews, Fife KY16 9ST, UK*

Received 27 March 1997; revised 8 May 1997; accepted 8 May 1997

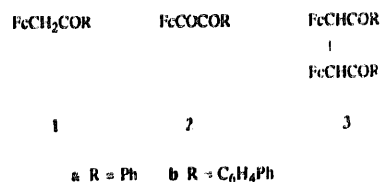
## Abstract

Oxidation of the ferrocenyl ketones  $\text{FcCH}_2\text{COR}$  **1** [ $\text{Fc} = (\text{C}_5\text{H}_5)_2\text{Fe}(\text{C}_5\text{H}_4)$ ; **a**  $\text{R} = \text{Ph}$ , **b**  $\text{R} = \text{C}_6\text{H}_4\text{Ph}$ ] with selenium(IV) oxide provides only modest yields of the corresponding 1,2-diketones  $\text{FcCOCOR}$  **2**, but substantial yields of the 1,4-butanediones  $\text{RCOCH}(\text{FcCH}(\text{Fc}))\text{COR}$  **3** resulting from C–C coupling. Compounds **3** exist in two diastereoisomeric forms, racemic and meso, and crystal structures are reported for *rac*-**3a**, *rac*-**3b** and *meso*-**3b**, as well as for **1b**. © 1997 Elsevier Science S.A.

## 1. Introduction

Manganese(IV) oxide is a well-established reagent for the oxidation of acyl ferrocenes  $\text{FcCOCH}_2\text{R}$  [ $\text{Fc} = (\text{C}_5\text{H}_5)_2\text{Fe}(\text{C}_5\text{H}_4)$ ] to 1,2-diketones  $\text{FcCOCOR}$  [1–3], and we have recently applied this reagent both to the oxidation of the ketones  $\text{FcCH}_2\text{COR}$ , isomeric with  $\text{FcCOCH}_2\text{R}$ , to  $\text{FcCOCOR}$  for  $\text{R} = \text{Ph}$ ,  $\text{C}_6\text{H}_4\text{Ph}$  and  $\text{Fc}$  [4,5] and to the oxidation of the diacyl ferrocene  $\text{Fc}(\text{C}_5\text{H}_4\text{COCH}_2\text{Ph})_2$  to the bis-1,2-diketone  $\text{Fc}(\text{C}_5\text{H}_4\text{COCOPh})_2$  [6]. Another widely-used reagent for the production of purely organic 1,2-diketones  $\text{RCOCOR}'$  by oxidation of  $\text{RCOCH}_2\text{R}'$  is selenium(IV) oxide: it was reported many years ago [2] that attempted application of the reagent to the oxidation of ferrocenyl mono-ketones led to complete decomposition, in a variety of solvents, although the solvents actually used were not specified. We have now re-investigated the use of

selenium(IV) oxide as an oxidant of ferrocenyl ketones and have found that oxidation of  $\text{FcCH}_2\text{COR}$  **1** (for  $\text{R} = \text{Ph}$  and  $\text{C}_6\text{H}_4\text{Ph}$ ) with  $\text{SeO}_2$  in acetic anhydride yields not only  $\text{FcCOCOR}$  **2** as a minor product, but also an unexpected coupled product  $(\text{FcCHCOR})_2$  **3** as the major product: we report here the application of  $\text{SeO}_2$  to a number of ferrocenyl systems, along with the crystal and molecular structures of racemic 2,3-diferrocenyl-1,4-diphenylbutane-1,4-dione,  $(\text{FcCHCOPh})_2$  **3a**, of both diastereoisomers, racemic and meso, of 2,3-diferrocenyl-1,4-bis(4-biphenyl)butane-1,4-dione,  $(\text{FcCHCOC}_6\text{H}_4\text{Ph})_2$  **3b**, and of ferrocenylmethyl(4-biphenyl)ketone  $\text{FcCH}_2\text{COC}_6\text{H}_4\text{Ph}$  **1b**.



<sup>\*</sup> Corresponding author.

## 2. Results and discussion

### 2.1. Oxidation of ferrocenyl ketones $FcCH_2COR$ by selenium(IV) oxide

Whereas manganese(IV) oxide readily oxidises the ferrocenyl ketones **1** to the 1,2-diketones **2** in practical yields, the use of the alternative oxidant selenium(IV) oxide, in refluxing acetic anhydride gives rather modest yields of the red 1,2-diketones **2**, along with a much bigger yield of less polar yellow materials. TLC of the oxidised material from both **1a** and **1b** indicated ready separation of the diketones **2** and showed in addition the presence of two yellow products in each case, having very similar  $R_f$  values in the case of **1a** and rather different  $R_f$  values for the products from **1b**. In the case of the products from **1a**, only one of the yellow components **3a** could be isolated pure, but both yellow products from **1b** have been isolated and characterised.

The  $^1H$  and  $^{13}C$  NMR spectra of compound **3a** both contained signals readily assignable to a mono-substituted ferrocene nucleus and a phenyl ring; in addition there was the expected CO resonance in the  $^{13}C$  spectrum. However, the  $CH_2$  signals for the precursor **1a** were replaced by signals characteristic of a CH group, while the substituted cyclopentadienyl ring of the ferrocene group gave four and five chemical shifts respectively in the  $^1H$  and  $^{13}C$  spectra, indicative of the presence of a neighbouring stereogenic centre rendering all five carbon atoms of this ring chemically and magnetically distinct. The simplest interpretation of these spectral data, in terms of oxidation of  $FcCH_2COPh$  to the hydroxyketone  $FcCH(OH)COPh$ , was however easily ruled out by the elemental analysis, and by the absence of  $\nu(OH)$  in the IR spectrum: moreover, the  $^1H$  and  $^{13}C$  chemical shifts of the unique CH group were scarcely consistent with the presence of both OH and CO groups as near-neighbours. An alternative formulation consistent with all the spectral and analytical data involves an oxidative coupling reaction to give the substituted butane-1,4-dione  $(FcCHCOPh)_2$  **3a** in which a new C–C bond has been generated; single-crystal X-ray diffraction (see below, Section 2.3) confirms that this formulation is correct, and that the isolated compound is the racemic form consisting of equal numbers of the RR and SS diastereoisomers.

During the work-up of compound **3a** it was apparent that before the final chromatographic separation each peak in the  $^1H$  and  $^{13}C$  NMR spectra was accompanied by a much smaller peak, of very similar chemical shift. Thus the major pattern, identical to that of the pure **3a** used for analytical, spectral and crystallographic characterisation, was mirrored by an entirely similar pattern with much lower intensities: integration of the  $^1H$  spectrum indicated a ratio of major to minor components of ca. 7:1. While we have been unable to isolate sufficient

of this minor component to characterise it, a reasonable hypothesis is that this material is in fact the RS ( $\equiv$  SR) diastereoisomer of **3a**, i.e. the meso form.

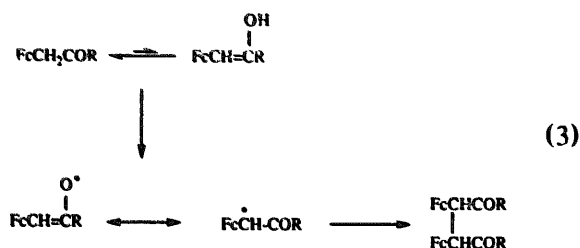
The yellow product formed by  $SeO_2$  oxidation of **1b** had  $^1H$  and  $^{13}C$  NMR spectra fully consistent with its formulation as **3b**. The crude yellow mixture exhibited a doubling of each signal in the  $^{13}C$  NMR spectrum, rather as for crude **3a**, but with the two components of each signal having intensities in the ratio ca. 2:1. Separation of this mixture on silica gel gave two pure products, both of which gave crystals suitable for single crystal X-ray analysis. The less polar and more abundant component proved to be the RR/SS diastereoisomer, denoted *rac*-**3b**, analogous to that characterised earlier for **3a**, and the more polar, less abundant, component proved to be the RS diastereoisomer, denoted *meso*-**3b**. Thus, the isolation and structural characterisation of both *rac*-**3b** and *meso*-**3b** rules out any possibility that the observed doublings in the NMR spectra of the crude products could be due to the occurrence of rotamers arising from restricted rotation about the newly-formed C–C bonds, and supports the supposition above that the minor compound accompanying the isolable **3a** is the corresponding meso diastereoisomer.

The formation of the coupled products **3** alongside the expected diketones **2** naturally raises the question of the reaction pathway, and two possibilities present themselves. The coupled products **3** could be intermediates on the pathway from **1** to **2** (Eq. (1)), or alternatively products **2** and **3** could be formed by divergent routes from **1** (Eq. (2)).



In order to test these possibilities, a sample of racemic **3a** was isolated and purified as already described, and then subjected to  $SeO_2$  oxidation under precisely the conditions employed for the oxidation of **1a**. The reaction was monitored by TLC but no **2a** was detected at any stage during a 5 h reaction time: aside from a small amount of decomposition, the **3a** initially added was recovered unchanged. Hence we conclude that compounds **2** and **3** do not lie on a common reaction pathway, and that Eq. (2) best represents their formation. While the details of the route from **1** to **3** in an oxidation reaction occurring primarily at the surface of the  $SeO_2$  must be somewhat speculative at this stage, a

reasonable possibility is the formation by hydrogen abstraction of a radical derived from the enol form of **1**, followed by radical coupling (Eq. (3)).



The formation of the coupled products **3** appears to be specific for  $\text{SeO}_2$  oxidations carried out using acetic anhydride as the reaction solvent. When the monoketone **1b** was subjected to  $\text{SeO}_2$  oxidation under similar conditions but using either 70% acetic acid or THF as solvent, there was no trace of any **3b** amongst the products: the isolable ferrocene product in each case was the diketone **2b**, in yields of 35% and 10%, respectively.

## 2.2. Oxidation of other ferrocenyl precursors by selenium(IV) oxide

Isomeric with the monoketones **1** are the acyl ferrocenes  $\text{FcCOCH}_2\text{R}$ ; oxidation of  $\text{FcCOCH}_2\text{Ph}$  to  $\text{FcCOCOPh}$  using  $\text{MnO}_2$  is known to be very slow [5], and its oxidation using  $\text{SeO}_2$  proves to be even less effective. No oxidation at all was observed when  $\text{FcCOCH}_2\text{Ph}$  and  $\text{SeO}_2$  were heated under reflux in acetic anhydride, glacial acetic acid, or 20% aqueous acetone, although traces of  $\text{FcCOCOPh}$  were formed in toluene.

However, oxidation of the phosphonium salt  $[\text{FcCH}(\text{COPh})\text{PPh}_3]^+ \text{I}^-$  with  $\text{SeO}_2$  in 20% aqueous

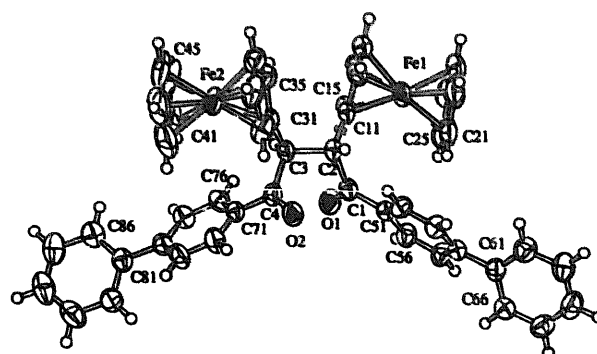


Fig. 2. View of the molecule of *rac*-**3b**, showing the atom-labelling scheme.

acetone yielded  $\text{FcCOCOPh}$  in 60% yield: this salt was previously used [5] as the precursor to the monoketone **1a** prior to oxidation to **2a** and/or **3a**. It is thus possible to eliminate the reduction of this salt to the labile  $\text{FcCH}_2\text{COPh}$ , and to use the salt directly in a more efficient route to the diketone **2a**. Again, the choice of solvent is critical: much poorer yields of **2a** (typically around 10%) were found in neat acetone or in methanol or ethanol, and in each case the diketone was accompanied by a comparable yield of the cleavage product  $\text{FcCHO}$ : in dichloromethane, this aldehyde was the sole isolable product.

## 2.3. Crystal and molecular structures of **3a**, **3b** and **1b**

The racemic form of compound **3a** crystallises in the triclinic space group  $P\bar{1}$  with two independent molecules

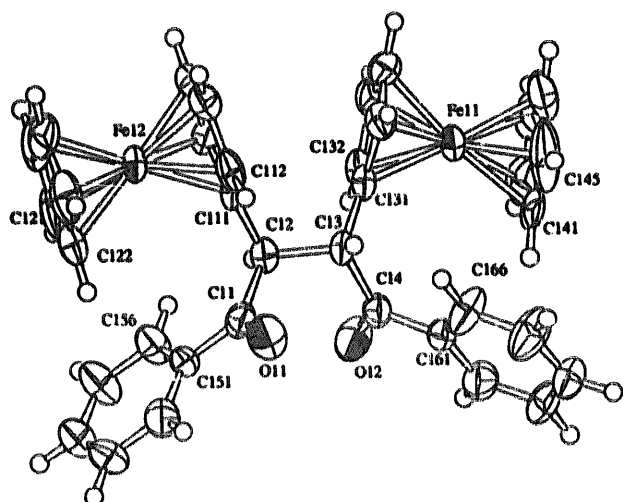


Fig. 1. View of molecule **1** in *rac*-**3a**, showing the atom-labelling scheme.

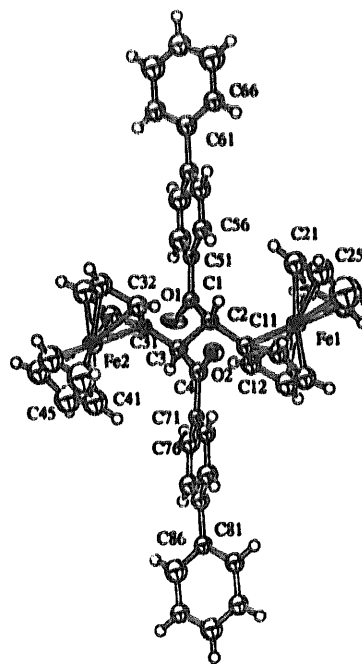


Fig. 3. View of the molecule of *meso*-**3b**, showing the atom-labelling scheme.

in the asymmetric unit. The structure analysis firstly confirms the constitution of compound **3a** and secondly, indicates that in each of the independent molecules the two stereogenic carbon atoms have the same stereochemistry, so that equal numbers of RR and SS molecules are accommodated by the centrosymmetric space group. For a molecule of type  $(Cabc)_2$  in which the two stereogenic carbon atoms are of the same hand, then if a, b and c represent mono-atomic substituents, there will be a two-fold rotation axis normal to the central C–C bond, regardless of the conformation adopted by the substituents: only if a, b and c represent poly-atomic substituents with internal conformational degrees of freedom can the molecular symmetry be less than  $C_2$ . In both independent molecules of *rac*-**3a** the torsional degrees of freedom, particularly those involving the aryl rings (Table 3) preclude exact  $C_2$  symmetry: however, Fig. 1 demonstrates clearly the approximate  $C_2$  axis, normal to the C12–C13 bond and lying approximately in the plane of the page. Not only is the molecular symmetry only approximately  $C_2$  but, in addition, the four independent  $-\text{CH}(\text{Fc})\text{COPh}$  fragments within the asymmetric unit are all conformationally distinct.

The structures of the two forms of compound **3b** show that these are indeed the racemic and meso diastereoisomers. *Rac*-**3b** is triclinic,  $P1$ , with equal numbers of RR and SS molecules in the unit cell and, just as found for *rac*-**3a**, the molecules have approximate but not precise two-fold rotational symmetry (Fig. 2 and Table 3). The meso form adopts a conformation (Fig. 3) which is approximately, though not precisely, centrosymmetric (Table 3), consistent with its RS configuration. In each of *rac*-**3a**, *rac*-**3b** and *meso*-**3b**, the molecules have the central  $\text{H}-\text{C}=\text{C}-\text{H}$  fragment in a *trans* conformation; this conformation uniquely minimises the steric repulsions between the four large substituents bonded to the central  $C_2$  fragment. All other staggered conformations require the four large substituents to be adjacent, while if the  $\text{H}-\text{C}=\text{C}-\text{H}$  is *trans*, only pairwise interactions occur between these large substituents.

When characterising the intermediates along the reaction pathway from  $[\text{FeCH}_2\text{PPh}_3]^+ \text{I}^-$  to  $\text{FeCOCOPh}$  [5], we were unable to obtain crystals of  $\text{FeCH}_2\text{COPh}$  suitable for single-crystal X-ray diffraction. While continued efforts to prepare suitable crystals of this compound have proved unsuccessful, we have now succeeded in obtaining a structure for the closely related compound **1b**,  $\text{FeCH}_2\text{COC}_6\text{H}_4\text{Ph}$ . The crystal quality for **1b** was consistently poor and a number of different crystals from different preparations were examined: eventually a data set was obtained at 200 K which provided a structure of sufficient quality to serve as definitive proof of constitution (Fig. 4).

In **3a**, **3b** and **1b**, the bond lengths and angles are all

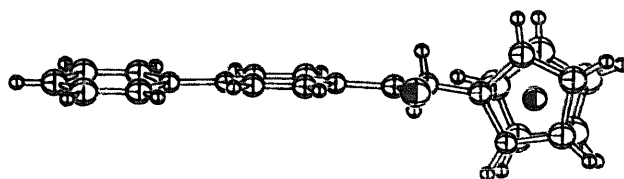


Fig. 4. View of the molecule of **1b**, viewed approximately along the five-fold axis of the ferrocene unit.

typical of their types [7,8]: there is evidence in **3a**, *rac*-**3b** and **1b** for large-amplitude librational motion of the unsubstituted cyclopentadienyl ring about the local five-fold axis of the ferrocene unit and relative to the rest of the structure, as observed in some other mono-substituted ferrocenes [9] and consistent with the very low barrier to rotation about the five-fold axis in ferrocene itself [10].

### 3. Experimental

NMR spectra were recorded at ambient temperatures, in  $\text{CDCl}_3$  solution unless stated otherwise, on a Bruker AM-300 spectrometer operating at 300.135 MHz for  $^1\text{H}$  and 75.469 MHz for  $^{13}\text{C}$ . Diethyl ether and light petroleum (b.p. 40–60°C) were dried over sodium wire. Ferrocenyl precursors were prepared as previously described [5].

#### 3.1. Oxidation of ferrocenyl ketones **1** by selenium(IV) oxide

Typically, the monoketone **1** (2.36 mmol) was added to a suspension of powdered selenium(IV) oxide (0.9 g, 8.1 mmol) in acetic anhydride (10  $\text{cm}^3$ ). This mixture was heated under reflux, and its composition was monitored by TLC; when the starting material **1** was all consumed (typically ca. 4 h), the mixture was cooled to ambient temperature and filtered, and the residue was washed with more acetic anhydride (5  $\text{cm}^3$ ). The combined filtrate and washings were hydrolysed with water (20  $\text{cm}^3$ ) and this solution was neutralised with sodium hydrogencarbonate. The neutral aqueous solution was extracted with dichloromethane ( $3 \times 50 \text{ cm}^3$ ); this extract was washed with water (100  $\text{cm}^3$ ) and dried ( $\text{MgSO}_4$ ), and the solvent was removed. Chromatography on silica with dichloromethane as eluent yielded yellow **3a** or **3b** (typical yields 55–70%) as mixtures of diastereoisomers (NMR), followed by red **2a** or **2b** (typical yields 10–15%). Further chromatography of the yellow components on silica using  $\text{CH}_2\text{Cl}_2$ /light petroleum (3:1 v/v) yielded for **3a**, firstly the pure racemic product, followed by a mixture of diastereoisomers, and for **3b** each diastereoisomer in pure form, accompanied by a mixed fraction. Anal. **3a** (*rac*/*meso*

mixture) Found: C 71.0, H 5.0;  $C_{36}H_{30}Fe_2O_2$  calc.: C 71.3, H 5.0%; **3b** (*rac/meso* mixture) Found: C 76.0, H 5.1;  $C_{48}H_{38}Fe_2O_2$  calc.: C 76.0, H 5.0%. NMR *rac-3a*,  $\delta$ (H) 3.42 (s, 1H), 3.95 (s, 1H), 4.12 (s, 1H) and 4.17 (s, 1H) ( $C_5H_4$ ); 3.60 (s, 5H,  $C_5H_5$ ); 4.78 (s, 1H, CH); 7.5–7.6 (m, 3H) and (8.1–8.2 (m, 2H) ( $C_6H_5$ );  $\delta$ (C) 51.9 (d, CH); 66.2 (d), 67.1 (d), 68.1 (d), 70.5 (d) and 82.1 (s) ( $C_5H_4$ ); 68.3 (d,  $C_5H_5$ ); 128.6 (d), 128.7 (d), 133.0 (d) and 138.0(s) ( $C_6H_5$ ); 199.6 (s, CO); *rac-3b*,  $\delta$ (C) 51.9 (d, CH); 66.9 (d), 67.8 (d), 68.7 (d), 71.0 (d) and 83.0 (s) ( $C_5H_4$ ); 68.9 (d,  $C_5H_5$ ); 126.9 (d), 127.2 (d), 128.0 (d), 128.8 (d), 130.0 (d), 136.7 (s), 140.0 (s) and 145.4 (s) ( $C_6H_5$ ); 199.1 (s, CO); *meso-3b*,  $\delta$ (C) 51.9 (d, CH); 66.8 (d), 67.7 (d), 68.6 (d), 70.9 (d) and 83.0 (s) ( $C_5H_4$ ); 68.8 (d,  $C_5H_5$ ); 127.2 (d), 127.3 (d), 128.5 (d), 129.2 (d), 129.4 (d), 136.7 (s), 149.8 (s) and 145.7 (s) ( $C_6H_5$ ); 199.1 (s, CO).

### 3.2. Oxidation of ferrocenyl( $\alpha$ -phenacyl)triphenylphosphonium iodide by selenium(IV) oxide

The phosphonium salt (4.0 g, 5.78 mmol) was added to a suspension of selenium(IV) oxide (7.0 g, 63 mmol)

in 20% aqueous acetone (50 cm<sup>3</sup>). The mixture was heated under reflux for 2h, cooled, and filtered; the solid residue was washed with dichloromethane (2  $\times$  50 cm<sup>3</sup>). Sufficient water and dichloromethane were added to the combined filtrate and washings until two layers separated. The organic layer was dried and the solvents removed. Chromatography on silica yielded the diketone **2a** (1.1 g, 3.46 mmol, 60%).

### 3.3. X-ray crystallography

Crystals of *rac-3a*, *meso-3b* and **1b** suitable for single-crystal X-ray diffraction were grown by slow evaporation of solutions in dichloromethane; suitable crystals of *rac-3b* were grown by slow evaporation of a solutions in acetone. Details of crystal data, data collection, structure solution and refinement are summarized in Table 1. In *rac-3a*, there are two independent molecules in the asymmetric unit and because of this, a careful check was made for possible missing symmetry using both the refined coordinates and the derived geometric parameters: none was found. In addition, the

Table 1  
Summary of crystal data, data collection, structure solution and refinement details

	<i>rac-3a</i>	<i>rac-3b</i>	<i>meso-3b</i>	<b>1b</b>
(a) Crystal data				
Empirical formula	$C_{36}H_{30}Fe_2O_2$	$C_{48}H_{38}Fe_2O_2$	$C_{48}H_{38}Fe_2O_2$	$C_{24}H_{20}FeO$
Molar mass	606.33	758.52	758.52	380.27
Colour, habit	yellow, needle	yellow, block	yellow needle	orange, plate
Crystal size, mm	0.3 $\times$ 0.07 $\times$ 0.07	0.50 $\times$ 0.30 $\times$ 0.25	0.45 $\times$ 0.10 $\times$ 0.05	0.35 $\times$ 0.25 $\times$ 0.05
Crystal system	Triclinic	Triclinic	Monoclinic	Monoclinic
<i>a</i> , Å	14.888(4)	12.617(5)	6.034(4)	42.64(1)
<i>b</i> , Å	18.583(6)	13.464(4)	28.68(3)	10.493(8)
<i>c</i> , Å	10.679(8)	11.870(3)	21.612(7)	7.880(10)
<i>a</i> , °	90.80(4)	98.91(3)	90	90
<i>b</i> , °	90.50(4)	105.27(2)	90.14(6)	93.3(1)
<i>c</i> , °	72.44(2)	104.88(3)	90	90
<i>V</i> , Å <sup>3</sup>	2816(2)	1825(1)	3740(3)	3521(6)
Space group	$P\bar{1}$	$P\bar{1}$	Cc	C2/c
<i>Z</i>	4 (two indep. molecules)	2	4	8
<i>F</i> (000)	1256	788	1576	1584
<i>d</i> <sub>calc</sub> , g cm <sup>-3</sup>	1.430	1.380	1.347	1.434
$\mu$ , mm <sup>-1</sup>	1.061	0.832	0.814	0.865
(b) Data acquisition <sup>a</sup>				
Temp., K	293(1)	293(1)	293(1)	200(1)
Unit-cell reflections ( $\theta$ -range °)	25 (15.0 to 25.0)	25 (24.0 to 25.0)	13 (6.8 to 11.7)	11 (6.5 to 15.6)
Max. $2\theta$ (°) for reflections	50.2	50.0	47.0	45.1
<i>hkl</i> range of reflections	0, 16; -21, 22; -12, 12	0, 14; -15, 15; -14, 13	0, 6; 0, 32; -24, 24	0, 45; 0, 11; -8, 8
Variation in 3 standard reflections	< 1.0%	< 1.0%	< 1.0%	< 1.0%
Reflections measured	10216	6706	3136	2496
Unique reflections	9797	6391	2829	2458
Reflections with $I > 3\sigma(I)$	5896	4599	1682	1484
(c) Structure solution and refinement <sup>b</sup>				
No. of variables in L.S.	722	469	227	235
<i>R</i> , <i>R</i> <sub>w</sub>	0.049, 0.052	0.040, 0.034	0.070, 0.060	0.090, 0.075
Density range in final $\Delta$ -map, e Å <sup>-3</sup>	-0.43, 0.37	-0.48, 0.40	-0.40, 0.92	-0.76, 1.02
Max. final shift/error ratio	0.052	0.134	0.093	0.064

<sup>a</sup> Data collection on a Rigaku AFC7S diffractometer with graphite monochromatised Mo-K $\alpha$  radiation ( $\lambda$  0.7107 Å).

<sup>b</sup> All calculations were made using the TeXsan suite of programs [11].

**Table 2**  
Fractional atomic coordinates and equivalent isotropic displacement parameters (Å<sup>2</sup>)

$U(\text{eq}) = (1/3) \sum_i \sum_j U_{ij} a_i^* a_j^* a_i a_j$				
Atom	x	y	z	$U(\text{eq})$
<b>Rac-3a</b>				
Fe(1)	0.34916(7)	0.33130(6)	0.83940(9)	0.0406(3)
Fe(12)	0.11579(7)	0.34729(6)	1.38982(9)	0.0402(3)
Fe(21)	-0.15868(6)	0.35936(6)	0.89522(9)	0.0378(3)
Fe(22)	-0.39082(7)	0.36774(6)	0.34839(9)	0.0439(3)
O(11)	0.3347(3)	0.1432(3)	1.3004(5)	0.067(2)
O(12)	0.2953(4)	0.1294(3)	0.9669(5)	0.069(2)
O(21)	-0.2259(4)	0.1567(3)	0.7745(5)	0.068(2)
O(22)	-0.1668(4)	0.1679(3)	0.4319(5)	0.076(2)
C(11)	0.2572(5)	0.1645(4)	1.2517(6)	0.044(2)
C(12)	0.2342(4)	0.2318(4)	1.1654(6)	0.037(2)
C(13)	0.3216(4)	0.2303(4)	1.0849(6)	0.035(2)
C(14)	0.3533(5)	0.1577(4)	1.0085(6)	0.042(2)
C(21)	-0.1639(5)	0.1799(4)	0.7347(6)	0.044(2)
C(22)	-0.1895(4)	0.2513(4)	0.6586(6)	0.035(2)
C(23)	-0.2722(4)	0.2533(4)	0.5685(6)	0.037(2)
C(24)	-0.2436(5)	0.1846(4)	0.4797(6)	0.046(2)
C(111)	0.2029(4)	0.3051(4)	1.2369(5)	0.035(2)
C(112)	0.2519(5)	0.3291(4)	1.3344(6)	0.050(2)
C(113)	0.2070(5)	0.4078(4)	1.3623(7)	0.054(3)
C(114)	0.1307(5)	0.4306(4)	1.2786(7)	0.057(3)
C(115)	0.1263(5)	0.3690(4)	1.2035(6)	0.044(2)
C(121)	0.0091(7)	0.3034(7)	1.4244(9)	0.086(4)
C(122)	0.0869(7)	0.2662(5)	1.4933(9)	0.076(3)
C(123)	0.1094(7)	0.3195(7)	1.5721(7)	0.075(3)
C(124)	0.0442(8)	0.3894(6)	1.5508(9)	0.076(4)
C(125)	-0.0169(6)	0.3812(7)	1.462(1)	0.088(4)
C(131)	0.2964(4)	0.2988(4)	1.0028(6)	0.037(2)
C(132)	0.2286(4)	0.3140(4)	0.9033(6)	0.044(2)
C(133)	0.2122(5)	0.3911(4)	0.8672(7)	0.055(3)
C(134)	0.2707(5)	0.4212(4)	0.9419(7)	0.052(2)
C(135)	0.3222(5)	0.3654(4)	1.0229(6)	0.045(2)
C(141)	0.456(1)	0.2482(6)	0.759(1)	0.109(5)
C(142)	0.3853(9)	0.2794(8)	0.6708(10)	0.097(5)
C(143)	0.3764(7)	0.3522(7)	0.6612(8)	0.079(4)
C(144)	0.4347(9)	0.3726(6)	0.740(1)	0.095(5)
C(145)	0.4872(6)	0.306(1)	0.800(1)	0.119(5)
C(151)	0.1846(5)	0.1254(4)	1.2754(6)	0.042(2)
C(152)	0.2059(5)	0.0663(4)	1.3579(7)	0.062(3)
C(153)	0.1387(7)	0.0304(4)	1.3866(8)	0.075(3)
C(154)	0.0513(7)	0.0541(5)	1.3346(9)	0.074(3)
C(155)	0.0302(6)	0.1111(5)	1.2518(8)	0.071(3)
C(156)	0.0961(5)	0.1474(4)	1.2224(7)	0.058(3)
C(161)	0.4557(5)	0.1235(4)	0.9795(6)	0.040(2)
C(162)	0.4806(5)	0.0678(4)	0.8863(8)	0.063(3)
C(163)	0.5733(6)	0.0366(5)	0.8522(8)	0.069(3)
C(164)	0.6418(6)	0.0607(5)	0.9073(8)	0.070(3)
C(165)	0.6181(6)	0.1145(5)	1.0009(9)	0.086(3)
C(166)	0.5254(5)	0.1467(5)	1.0356(7)	0.064(3)
C(211)	-0.2173(4)	0.3193(4)	0.7415(6)	0.036(2)
C(212)	-0.3008(5)	0.4073(4)	0.8883(7)	0.052(2)
C(214)	-0.2564(5)	0.4436(4)	0.8065(7)	0.047(2)
C(215)	-0.2046(5)	0.3902(4)	0.7168(6)	0.042(2)
C(221)	-0.0281(6)	0.2886(5)	0.9376(9)	0.072(3)
C(222)	-0.0879(7)	0.2976(6)	1.0401(9)	0.082(4)
C(223)	-0.1178(6)	0.3739(6)	1.0728(7)	0.072(3)
C(224)	-0.0802(6)	0.4137(5)	0.9944(9)	0.067(3)
C(225)	-0.0239(5)	0.3623(6)	0.9113(8)	0.072(3)
C(231)	-0.3000(4)	0.3262(4)	0.4978(6)	0.037(2)
C(232)	-0.3729(4)	0.3922(4)	0.5326(6)	0.040(2)

**Table 2 (continued)**

$U(\text{eq}) = (1/3) \sum_i \sum_j U_{ij} a_i^* a_j^* a_i a_j$				
Atom	x	y	z	$U(\text{eq})$
<b>Rac-3a</b>				
C(233)	-0.3695(5)	0.4523(4)	0.4577(7)	0.048(2)
C(234)	-0.2959(5)	0.4269(5)	0.3754(7)	0.059(3)
C(235)	-0.2529(5)	0.3476(4)	0.3966(6)	0.049(2)
C(241)	-0.425(1)	0.2866(6)	0.250(1)	0.102(5)
C(242)	-0.496(1)	0.322(1)	0.321(1)	0.144(8)
C(243)	-0.5222(7)	0.4006(9)	0.281(1)	0.117(5)
C(244)	-0.464(1)	0.4023(7)	0.186(1)	0.095(4)
C(245)	-0.4054(7)	0.3342(9)	0.1713(9)	0.093(4)
C(251)	-0.0640(5)	0.1410(4)	0.7668(6)	0.042(2)
C(252)	-0.0437(5)	0.1013(4)	0.8765(7)	0.057(3)
C(253)	0.0488(6)	0.0668(4)	0.9129(8)	0.066(3)
C(254)	0.1212(6)	0.0714(5)	0.8404(9)	0.068(3)
C(255)	0.1020(6)	0.1075(5)	0.7289(8)	0.075(3)
C(256)	0.0099(5)	0.1425(4)	0.6919(7)	0.056(2)
C(261)	-0.3108(5)	0.1404(4)	0.4531(6)	0.042(2)
C(262)	-0.2894(5)	0.0882(5)	0.3569(7)	0.064(3)
C(263)	-0.3493(7)	0.0454(5)	0.3269(9)	0.084(4)
C(264)	-0.4324(7)	0.0568(5)	0.3918(10)	0.087(4)
C(265)	-0.4534(7)	0.1078(6)	0.4893(10)	0.093(4)
C(266)	-0.3925(6)	0.1503(5)	0.5204(8)	0.070(3)
<b>Rac-3b</b>				
Fe(1)	0.93855(4)	0.54355(4)	0.21572(5)	0.0516(2)
Fe(2)	0.78740(5)	-0.00855(4)	0.07288(5)	0.0625(2)
O(1)	0.7856(2)	0.3626(2)	0.4282(2)	0.0603(8)
O(2)	0.5808(2)	0.1596(2)	0.2391(2)	0.0634(8)
C(1)	0.7373(3)	0.3688(2)	0.3275(3)	0.0447(10)
C(2)	0.7662(3)	0.3164(2)	0.2214(3)	0.0403(9)
C(3)	0.7750(3)	0.2058(2)	0.2361(3)	0.0404(9)
C(4)	0.6760(3)	0.1501(2)	0.2788(3)	0.0465(10)
C(11)	0.8793(3)	0.3856(2)	0.2161(3)	0.0415(9)
C(12)	0.9097(3)	0.3987(2)	0.1112(3)	0.052(1)
C(13)	1.0279(3)	0.4587(3)	0.1470(4)	0.060(1)
C(14)	1.0705(3)	0.4848(3)	0.2728(4)	0.062(1)
C(15)	0.9799(3)	0.4408(3)	0.3168(3)	0.054(1)
C(21)	0.8160(4)	0.6194(3)	0.2106(6)	0.089(2)
C(22)	0.8608(5)	0.6304(3)	0.1150(5)	0.094(2)
C(23)	0.9791(5)	0.6819(3)	0.1637(5)	0.090(2)
C(24)	1.0093(4)	0.7018(3)	0.2876(5)	0.092(2)
C(25)	0.9082(5)	0.6624(3)	0.3181(5)	0.096(2)
C(31)	0.7675(3)	0.1382(2)	0.1184(3)	0.0446(10)
C(32)	0.6654(3)	0.0650(3)	0.0321(4)	0.067(1)
C(33)	0.6924(4)	0.0272(3)	-0.0706(4)	0.076(1)
C(34)	0.8086(4)	0.0747(3)	-0.0510(4)	0.071(1)?
C(35)	0.8570(3)	0.1438(3)	0.0660(3)	0.053(1)
C(41)	0.8439(9)	-0.0637(6)	0.2181(6)	0.150(4)
C(42)	0.7353(8)	-0.1275(5)	0.1534(9)	0.153(4)
C(43)	0.7405(7)	-0.1694(4)	0.0372(6)	0.131(3)
C(44)	0.8512(7)	-0.1282(5)	0.0351(5)	0.120(3)
C(45)	0.9199(5)	-0.0619(4)	0.1495(6)	0.128(3)
C(51)	0.6541(3)	0.4305(2)	0.3086(3)	0.0423(9)
C(52)	0.5704(3)	0.4167(2)	0.1996(3)	0.049(1)
C(53)	0.4980(3)	0.4791(3)	0.1880(3)	0.052(1)
C(54)	0.5079(3)	0.5575(2)	0.2851(3)	0.046(1)
C(55)	0.5898(3)	0.5695(3)	0.3943(3)	0.055(1)
C(56)	0.6619(3)	0.5075(3)	0.4065(3)	0.053(1)
C(61)	0.4351(3)	0.6288(2)	0.2735(3)	0.049(1)
C(62)	0.4140(3)	0.6721(3)	0.1747(3)	0.064(1)
C(63)	0.3528(3)	0.7443(3)	0.1681(4)	0.072(1)
C(64)	0.3113(3)	0.7726(3)	0.2592(4)	0.069(1)
C(65)	0.3301(3)	0.7298(3)	0.3571(4)	0.066(1)
C(66)	0.3921(3)	0.6585(3)	0.3648(3)	0.057(1)

Table 2 (continued)

$U(\text{eq}) = (1/3) \sum_i \sum_j U_{ij} a_i^* a_j^* a_i a_j$				
Atom	x	y	z	$U(\text{eq})$
<b>Rac-3b</b>				
C(71)	0.6963(3)	0.0822(2)	0.3648(3)	0.0441(10)
C(72)	0.6020(3)	0.0005(3)	0.3631(3)	0.059(1)
C(73)	0.6166(3)	-0.0678(3)	0.4376(3)	0.063(1)
C(74)	0.7235(3)	-0.0563(2)	0.5169(3)	0.049(1)
C(75)	0.8166(3)	0.0288(3)	0.5224(3)	0.052(1)
C(76)	0.8030(3)	0.0962(2)	0.4466(3)	0.050(1)
C(81)	0.7376(3)	-0.1344(2)	0.5905(3)	0.051(1)
C(82)	0.6546(3)	-0.1761(3)	0.6412(3)	0.061(1)
C(83)	0.6653(4)	-0.2533(3)	0.7041(3)	0.077(2)
C(84)	0.7579(4)	-0.2903(3)	0.7164(4)	0.081(2)
C(85)	0.8412(4)	-0.2496(3)	0.6677(4)	0.077(1)
C(86)	0.8315(3)	-0.1726(3)	0.6040(3)	0.064(1)
<b>Meso-3b</b>				
Fe(1)	0.1724	0.14577(9)	0.8419	0.0380(9)
Fe(2)	0.4415(6)	0.16587(9)	0.4925(2)	0.0415(10)
O(1)	0.659(2)	0.1906(4)	0.7153(7)	0.047(5)
O(2)	-0.031(2)	0.1168(4)	0.6198(6)	0.035(4)
C(1)	0.461(3)	0.2036(6)	0.7132(8)	0.026(5)
C(2)	0.280(3)	0.1683(6)	0.6988(9)	0.030(5)
C(3)	0.339(3)	0.1421(6)	0.6370(9)	0.032(5)
C(4)	0.158(3)	0.1046(7)	0.6228(8)	0.034(5)
C(11)	0.263(4)	0.1316(7)	0.7521(9)	0.036(5)
C(12)	0.433(3)	0.1181(7)	0.7922(9)	0.043(6)
C(13)	0.344(4)	0.0855(7)	0.832(1)	0.055(6)
C(14)	0.109(4)	0.0788(7)	0.8175(9)	0.051(6)
C(15)	0.058(3)	0.1098(7)	0.7668(9)	0.043(6)
C(21)	0.116(4)	0.2150(7)	0.8586(10)	0.053(6)
C(22)	0.283(4)	0.1915(9)	0.906(1)	0.072(8)
C(23)	0.116(4)	0.1572(7)	0.9330(10)	0.051(6)
C(24)	-0.069(6)	0.164(1)	0.900(2)	0.12(1)
C(25)	-0.071(4)	0.1934(9)	0.861(1)	0.076(8)
C(31)	0.356(3)	0.1751(6)	0.5844(8)	0.024(5)
C(32)	0.179(3)	0.1927(7)	0.5428(9)	0.043(6)
C(33)	0.281(4)	0.2280(7)	0.5039(10)	0.052(6)
C(34)	0.513(4)	0.2324(8)	0.521(1)	0.061(7)
C(35)	0.551(4)	0.2013(8)	0.5686(10)	0.045(6)
C(41)	0.434(4)	0.0979(8)	0.467(1)	0.066(7)
C(42)	0.315(5)	0.123(1)	0.427(1)	0.098(10)
C(43)	0.430(4)	0.1545(8)	0.401(1)	0.071(8)
C(44)	0.663(4)	0.1523(7)	0.424(1)	0.058(7)
C(45)	0.674(5)	0.1167(9)	0.469(1)	0.078(8)
C(51)	0.408(3)	0.2529(6)	0.7242(8)	0.026(4)
C(52)	0.578(4)	0.2815(8)	0.7500(10)	0.051(7)
C(53)	0.529(4)	0.3271(8)	0.759(1)	0.051(7)
C(54)	0.327(3)	0.3489(6)	0.7449(8)	0.035(5)
C(55)	0.164(3)	0.3200(7)	0.7207(9)	0.043(6)
C(56)	0.194(3)	0.2729(6)	0.7103(9)	0.036(5)
C(61)	0.280(3)	0.4007(6)	0.7533(9)	0.040(5)
C(62)	0.458(3)	0.4310(7)	0.7402(9)	0.044(6)
C(63)	0.411(4)	0.4797(8)	0.747(1)	0.060(7)
C(64)	0.221(4)	0.4946(7)	0.767(1)	0.051(6)
C(65)	0.043(4)	0.4659(9)	0.783(1)	0.068(8)
C(66)	0.090(3)	0.4171(7)	0.7755(9)	0.042(6)
C(71)	0.224(3)	0.0547(6)	0.6106(8)	0.024(4)
C(72)	0.067(3)	0.0270(7)	0.5857(8)	0.036(5)
C(73)	0.109(3)	-0.0204(7)	0.5766(9)	0.044(6)
C(74)	0.307(3)	-0.0402(6)	0.5942(8)	0.033(5)
C(75)	0.477(4)	-0.0127(7)	0.620(1)	0.042(6)
C(76)	0.417(3)	0.0345(7)	0.6283(9)	0.044(6)
C(81)	0.346(3)	-0.0913(6)	0.5860(8)	0.032(5)

Table 2 (continued)

$U(\text{eq}) = (1/3) \sum_i \sum_j U_{ij} a_i^* a_j^* a_i a_j$				
Atom	x	y	z	$U(\text{eq})$
<b>Meso-3b</b>				
C(82)	0.189(3)	-0.1237(6)	0.6020(9)	0.037(5)
C(83)	0.224(3)	-0.1713(7)	0.5960(9)	0.041(5)
C(84)	0.421(4)	-0.1869(7)	0.5757(9)	0.050(6)
C(85)	0.583(3)	-0.1559(7)	0.5600(9)	0.037(6)
C(86)	0.553(4)	-0.1077(8)	0.567(1)	0.053(7)
<b>1b</b>				
Fe(1)	0.55865(5)	0.2572(2)	0.1280(2)	0.0368(6)
O(1)	0.6397(2)	0.4713(9)	0.464(1)	0.054(4)
C(1)	0.5952(4)	0.338(1)	0.269(2)	0.038(5)
C(2)	0.5721(4)	0.281(2)	0.375(2)	0.054(6)
C(3)	0.5414(4)	0.338(2)	0.342(2)	0.052(6)
C(4)	0.5453(4)	0.434(1)	0.214(2)	0.047(6)
C(5)	0.5784(4)	0.434(1)	0.174(2)	0.036(5)
C(6)	0.5786(5)	0.125(2)	-0.014(2)	0.065(7)
C(7)	0.5536(7)	0.070(2)	0.076(2)	0.070(7)
C(8)	0.5260(5)	0.129(2)	0.045(3)	0.077(8)
C(9)	0.5304(5)	0.215(3)	-0.081(3)	0.104(10)
C(10)	0.5625(7)	0.221(1)	-0.118(2)	0.081(7)
C(11)	0.6279(3)	0.307(1)	0.261(2)	0.035(5)
C(12)	0.6497(4)	0.390(1)	0.370(2)	0.036(5)
C(13)	0.6843(4)	0.375(1)	0.361(1)	0.027(4)
C(14)	0.6991(4)	0.287(1)	0.256(2)	0.039(5)
C(15)	0.7313(4)	0.280(1)	0.247(2)	0.035(5)
C(16)	0.7505(3)	0.363(1)	0.338(1)	0.027(4)
C(17)	0.7373(4)	0.447(1)	0.448(2)	0.033(5)
C(18)	0.7055(4)	0.453(1)	0.456(2)	0.037(5)
C(19)	0.7841(4)	0.358(1)	0.325(1)	0.029(4)
C(20)	0.7996(4)	0.267(2)	0.232(1)	0.043(5)
C(21)	0.8326(4)	0.264(2)	0.225(2)	0.046(5)
C(22)	0.8520(4)	0.354(2)	0.305(2)	0.051(6)
C(23)	0.8376(4)	0.445(2)	0.399(2)	0.050(6)
C(24)	0.8048(4)	0.447(1)	0.408(2)	0.044(5)

Laue group for *rac-3a* was confirmed as  $\bar{1}$ , and the lack of any systematic absences in the diffraction data was checked and confirmed. For all compounds, azimuthal scans of a range of reflections indicated that there was no need for any absorption corrections to be applied. Crystals of *meso-3b* did not diffract strongly, and even for the best crystal employed it was apparent that no further 'observed' data were being collected at  $2\theta > 47^\circ$ ; consequently data-collection was terminated at that point. The E statistics for *meso-3b* confirmed the absence of a centre of inversion, and the Laue group was confirmed as  $2/m$ , supporting the space group assignment as Cc. Because of the restricted number of data for this compound, only the iron and oxygen atoms were refined anisotropically. For compound **1b**, the crystal quality was consistently poor, and six different crystals selected from three separate preparations were investigated: the data set collected at 200 K from the best of these was not of high quality, but is probably the best that can be achieved for this compound. Although the refined bond lengths and angles all have satisfactory

Table 3  
Selected molecular dimensions (Å, °)

<i>Rac-3a</i>	Molecule 1	Molecule 2
Cn1–On1	1.215(8)	1.212(7)
Cn4–On4	1.217(7)	1.207(8)
Cn1–Cn2	1.517(9)	1.512(9)
Cn2–Cn3	1.559(8)	1.548(8)
Cn3–Cn4	1.517(8)	1.533(9)
Cn2–Cn11	1.500(8)	1.487(8)
Cn3–Cn31	1.505(9)	1.504(9)
On1–Cn1–Cn2	119.2(6)	119.5(6)
On1–Cn1–Cn51	121.1(6)	120.1(6)
Cn2–Cn1–Cn51	119.7(6)	120.2(6)
On2–Cn4–Cn3	120.0(6)	118.6(6)
On2–Cn4–Cn61	120.5(6)	121.4(6)
Cn3–Cn4–Cn61	119.5(6)	120.0(6)
Cn1–Cn2–Cn3–Cn4	58.5(7)	–59.7(7)
On1–Cn1–Cn2–Cn3	38.0(8)	–40.1(8)
Cn51–Cn1–Cn2–Cn3	–141.7(6)	143.5(6)
Cn2–Cn1–Cn51–Cn52	–177.5(6)	149.7(7)
Cn2–Cn1–Cn51–Cn56	–0.3(10)	–30(1)
On2–Cn4–Cn3–Cn2	35.2(8)	–44.7(9)
Cn61–Cn4–Cn3–Cn2	–147.9(5)	136.0(6)
Cn3–Cn4–Cn61–Cn62	–165.3(6)	168.6(7)
Cn3–Cn4–Cn61–Cn66	11(1)	–11(1)
<b>Compound 3b</b>	<i>Rac-3b</i>	<i>Meso-3b</i>
C1–O1	1.217(3)	1.26(2)
C4–O2	1.217(4)	1.19(2)
C1–C2	1.522(4)	1.52(2)
C2–C3	1.554(4)	1.58(2)
C3–C4	1.533(4)	1.57(2)
C1–C51	1.491(4)	1.47(2)
C4–C71	1.488(4)	1.51(3)
O1–C1–C2	119.3(3)	119(1)
O1–C1–C51	120.4(3)	119(1)
C2–C1–C51	120.3(3)	121(1)
O2–C4–C3	119.4(3)	118(1)
O2–C4–C71	120.8(3)	121(1)
C3–C4–C71	119.8(3)	120(1)
C1–C2–C3–C4	42.6(3)	178(1)
O1–C1–C2–C3	42.1(4)	–53(1)
C51–C1–C2–C3	–140.2(3)	126(1)
C2–C1–C51–C52	22.8(5)	166(1)
C2–C1–C51–C56	–156.5(3)	–12(2)
O2–C4–C3–C2	38.2(4)	55(2)
C71–C4–C3–C2	–143.8(3)	–127(1)
C3–C4–C71–C72	–153.2(3)	–165(1)
C3–C4–C71–C76	27.1(5)	21(2)

values, their metrical precision is not high with typical e.s.d.s for bond lengths and angles of  $\pm 0.02$  Å and  $\pm 1^\circ$ , respectively.

### 3.4. Structure solution and refinement

All structures were solved by direct methods, and refined by full-matrix least squares on F using observed data [11]. All hydrogen atoms were included in the refinements as riding atoms in geometrically-idealised positions, with  $d(\text{C–H}) = 0.95$  Å. Refined atom coordinates are given in Table 2, and selected geometric parameters for compounds **3a** and **3b** in Table 3. Fig. 1 shows a perspective views of one of the two independent molecules in the structure of compound **3a**, Fig. 2 and Fig. 3 show the molecules of *rac-3b* and *meso-3b*, and Fig. 4 shows compound **1b**. Tables of H-atom coordinates and displacement parameters have been deposited at the Cambridge Crystallographic Data Centre.

### Acknowledgements

S.Z.A. thanks the Committee of Vice-Chancellors and Principals (UK), and the University of St Andrews for financial support.

### References

- [1] K.L. Rinehart, A.F. Ellis, C.J. Michejda, P.A. Kittle, *J. Am. Chem. Soc.* **82** (1960) 4112.
- [2] M.D. Rausch, A. Siegel, *J. Org. Chem.* **33** (1968) 4545.
- [3] A.J. Fattadi, *Synthesis* (1976) 133.
- [4] C. Glidewell, M.J. Gottfried, J. Trotter, G. Ferguson, *Acta Cryst. C* **52** (1996) 773.
- [5] C. Glidewell, S.Z. Ahmed, M. Gottfried, P. Lightfoot, B.J.L. Royles, J.P. Scott, J. Wonnemann, *J. Organomet. Chem.*, in press.
- [6] G. Ferguson, C. Glidewell, B.J.L. Royles, D.M. Smith, *Acta Cryst. C* **52** (1996) 2465.
- [7] F.H. Allen, O. Kennard, D.G. Watson, L. Brammer, A.G. Orpen, R. Taylor, *J. Chem. Soc., Perkin Trans. 2* (1987) S1.
- [8] A.G. Orpen, L. Brammer, F.H. Allen, O. Kennard, D.G. Watson, R. Taylor, *J. Chem. Soc., Dalton Trans.* (1989) S1.
- [9] G. Ferguson, C. Glidewell, J.P. Scott, *Acta Cryst. C* **51** (1995) 1989.
- [10] A. Haaland, J.E. Nilsson, *Acta Chem. Scand.* **22** (1968) 2653.
- [11] TeXsan Crystal Structure Analysis Package, 1985 and 1992, Molecular Structure Corporation, The Woodlands, TX 77381, USA.